Vol. 01, No. 01, July 2025 : 11-19 Received: June 24, 2025. Revised: July 10, 2025.

International Journal of Electrical and Intelligent Engineering

Blind Spot Detection to Prevent Serious Accidents for Children in Cyclists

Utari Sanaba[1]* Virhan Mujahid Syufie[2] Rasyeedah Binti Mohd Othman[3]
Muhammad Richard Dzaki Dharma[4]

[1,4]*Universitas Islam Negeri Maulana Malik Ibrahim Malang, Indonesia*
[2]*Politeknik Elektronika Negeri Surabaya, Indonesia*
[3]*Universiti Teknologi PETRONAS, Malaysia*
* Corresponding author's Email: utarisanaba@uin-malang.ac.id

Abstract: Bicycles are used not only for transportation but also as a means of exercise. However, the lack of safety features increases the risk of accidents and theft, especially for children. This research develops a bicycle safety system using ultrasonic sensors to detect objects in blind spots and provide early warnings when the rider changes lanes. The system includes a smart lock and location monitoring, controlled via an application using the TCP/IP protocol with a SIM900A module. Testing showed successful GPS data transmission with very low error rates: 0.0012614% for latitude and 5.413E-05% for longitude. The blind spot detector accurately measured the distance of walls and nearby vehicles with an accuracy of 92.77%. The safety system—consisting of the smart lock and LED indicators—was successfully activated when a vehicle entered the cyclist's blind spot, enhancing protection and awareness for the rider.

Keywords: SIM900A, Blind spot detector, Ultrasonic sensor, Smart lock, GPS

1. Introduction

Bicycles have become one of the most popular modes of transportation by the public, both as a form of exercise and as a means of commuting to work. Since the Covid-19 pandemic, there has been a significant increase in bicycle users. One of the causes of this surge is the heightened public awareness of adopting a healthy lifestyle and the World Health Organization's (WHO) recommendation to avoid crowds that can occur in public transportation [1-2]. Cycling can have positive impacts on physical and mental health, increase feelings of happiness, and support overall improvement in quality of life, especially for those who are physically inactive or overweight [3-4]. However, the rise in bicycle usage also brings a potential increase in cyclist accidents.

According to accident data from the Central Statistics Agency of DKI Jakarta Province (2021), there has been an increase in the number of bicycle-related accidents in the province. The number of these accidents is significantly higher compared to the total accidents involving public transportation such as city buses. Additionally, in 2020, the Bike to Work (B2W) community recorded 29 cycling-related accidents between January and June 2020 [5]. This increase in accident rates is a concerning issue, especially in urban areas with high transportation mobility [6].

The provision of bicycle lanes, compliance, and safety standards are priority programs to ensure cyclist safety [5]. However, due to high mobility, bike lanes often become disorganized and not exclusive to bicycles, making road safety a concern for every individual [7-8]. Meeting bicycle safety standards is critical to prevent accidents, especially for children with autism who use cycling as a means to improve executive function [9].

Cyclist accidents are commonly caused by collisions in blind spot areas. A blind spot is an area around a vehicle that cannot be seen by the driver, even with the help of mirrors [10]. These blind spot areas pose a significant danger to road users as they often create confusing visual illusions. These illusions can mislead cyclists or other road users into thinking the area is clear of vehicles or obstacles, when in fact, it is not visible to the driver [11]. The invisibility of certain areas around a vehicle often causes drivers to be unaware of the presence of other road users. To address this issue, the use of blind spot detection technology is crucial, as it can provide early warnings to drivers about objects or vehicles in these zones, thereby significantly reducing the risk of collisions [12].

Parental concerns about letting their children cycle, as well as safety concerns for daily cyclists, can be addressed with a blind spot detector that provides automatic warnings to help minimize side and blind spot collisions. This study proposes a

International Journal of Electrical and Intelligent Engineering

system designed to monitor the bicycle's position and incorporates a bike lock integrated into the bicycle frame, which can be managed and monitored via an application to prevent bicycle theft and allow parents to track their child's bicycle. The system also features a blind spot detector to help avoid side collisions due to sudden lane changes, using LED and sound indicators to alert the cyclist to the presence of other vehicles on the rear and right side of the bike.

The novelty of this study lies in the integration of three critical safety features into a single, compact system specifically designed for bicycles: a blind spot detection mechanism, a smart anti-theft bike lock, and a real-time GPS monitoring system. While previous research has explored these technologies separately, this study uniquely combines them into one unified framework that addresses not only accident prevention through early warning alerts but also security and parental monitoring concerns. Moreover, the application-based control using the TCP/IP protocol and SIM900A module introduces a more accessible and scalable solution for urban environments. This comprehensive integration offers a new paradigm in bicycle safety systems, especially for vulnerable users such as children and individuals with special needs.

2. Method

2.1 Design System

The system design in this study is divided into four parts: sensor reading, input parameter data processing using a microcontroller, GPS monitoring results, and padlock control, as shown in Fig. 1.

This system operates in two modes controlled by a mobile device: the first is driving mode, and the second is parking mode. In driving mode, input from the JSN-SR04T ultrasonic sensor will be displayed on the indicator if it reaches a predefined threshold based on the database. The U-Blox Neo 6M GPS will collect longitude and latitude data every minute and store it in the micro buffer. The SIM900 module will send the location data previously stored in the buffer, and the system will then check the condition stored in the database—either driving or parking. The mobile device can set the bicycle's condition (driving or parking mode) and also display the bicycle's location, which is directly integrated with a website and stored in the database.

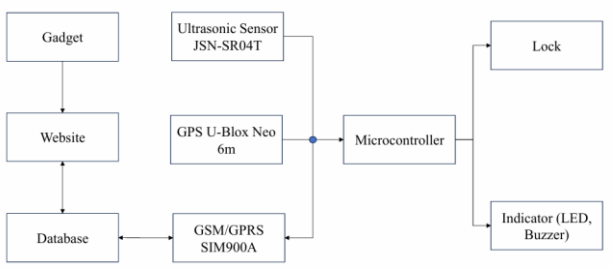

Figure 1. System block diagram

2.2 Flowchart

The flowchart in this study begins from the start and proceeds through several condition checks to determine the mode selected by the user, as shown in Fig. 2.

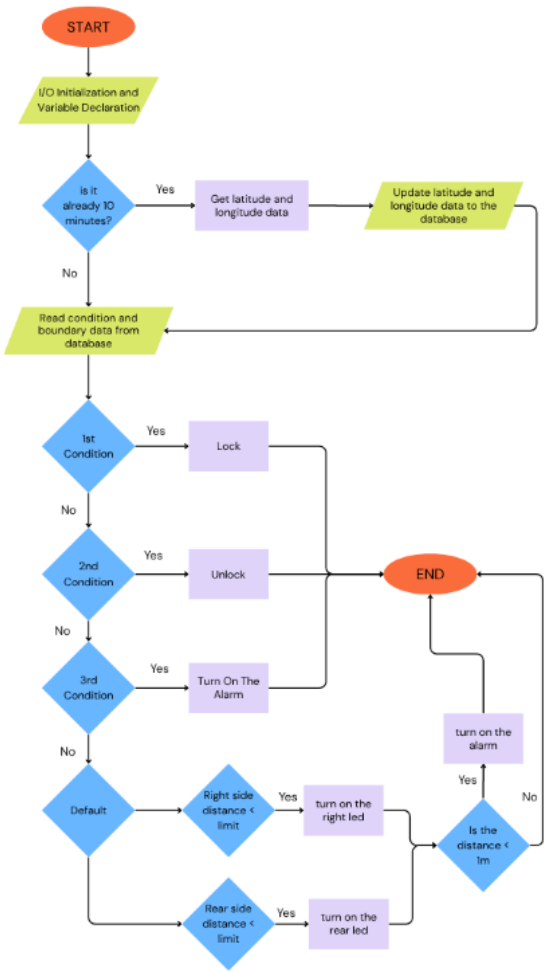

Figure 2. Flowchart

The flowchart in Fig. 2 illustrates how the system operates, starting with the initialization of I/O pins—both input and output—as well as the variables

International Journal of Electrical and Intelligent Engineering

used in the system. Then, the system checks whether 10 minutes have elapsed; if so, the GPS latitude and longitude values will be sent to the database. If less than 10 minutes have passed, the device will read data from the database and proceed to a condition check to determine the output for Condition 1, Condition 2, or Condition 3. The data is read continuously, and in the default condition, the system reads data every 2 minutes.

2.3 Web-based Application

The system in this study uses a website to monitor the location of the bicycle, set a safe riding distance—especially when the rider is a child so that parents can supervise them—and control the lock/unlock mechanism, as shown in Fig. 3.

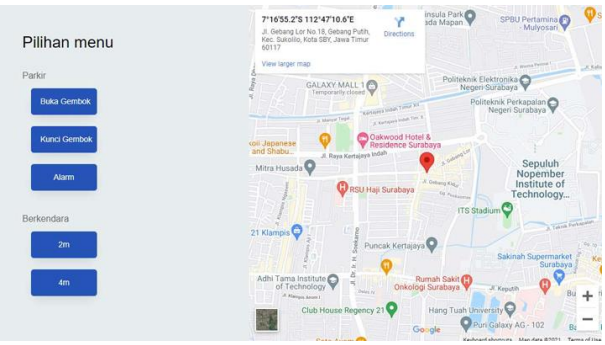

Figure 3. Website design

Fig. 3 above shows the website interface used to control the system, which can be accessed via a mobile device. It features five buttons, each with a specific function to help the user maintain the security of the bicycle. The unlock button is used to open the padlock, the lock button is used to lock the bicycle, and the alarm button activates an alarm for three seconds to help locate the bicycle in a crowd or parking area. In addition to these, there are also buttons to set the maximum riding distance when the bicycle is used by children—namely, the 2-meter button and the 4-meter button, which set the distance limit to 2 meters or 4 meters, respectively.

2.4 Hardware Design

The placement of the padlock and detector is adjusted according to the bicycle used, as shown in Fig. 4.

The hardware implementation for this study consists of two devices. The first device is a security padlock installed on the bicycle frame to secure the bike. This padlock includes a solenoid lock and a 6 mm-thick, 50 cm-long sling cable. The second device is a blind spot detector used to detect the cyclist's blind spots. It is mounted at the rear of the bicycle at a height of 40 cm from the ground. This placement considers the appropriate height to detect objects behind and on the right side of the bicycle, as shown in Fig. 4, arrow 3. The detector box measures 15 x 10 x 7 cm, as shown in Fig. 5.

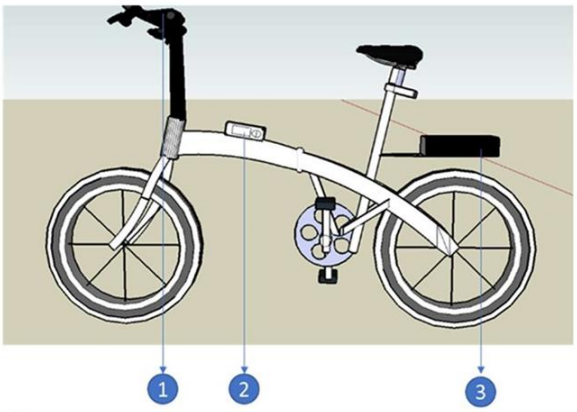

1 => Blind Spot Indicator
2 => Lock
3 => Control and Detector Box

Figure 4. Hardware placement

Fig. 5 shows the final design of the detector box, with detailed dimensions of 7.1 cm in width, 4.8 cm in length, and 3.5 cm in height. The angle difference between the rear and right-side sensors is set at 25 degrees. This angle must be precise to ensure that the detection ranges of the rear and side sensors do not overlap, which could cause incorrect sensor readings. The box is made from 2 mm filament material to ensure both structural strength and precise sensor angle alignment.

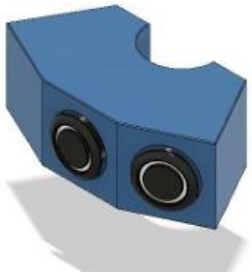

Figure 5. Detector design

Fig. 6 shows the lock design, with dimensions as follows: A (diameter) = 0.8 cm, B = 0,6 cm, C = 1 cm, D = 7 cm, E = 0,9 cm and F = 0,2 cm. The

International Journal of Electrical and Intelligent Engineering

padlock is made of 3 mm thick acrylic to ensure the design is secure and durable. It is mounted on the bicycle frame to reduce the risk of breakage.

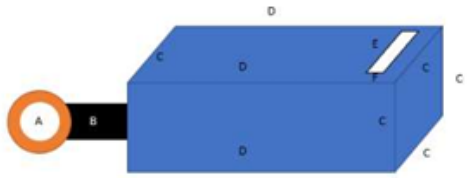

Figure 6. Lock design

The schematic circuit for the detector, padlock, and microcontroller is shown in Fig. 7. The circuit uses two ultrasonic sensors connected to a microcontroller, along with a SIM900 module and a U-Blox Neo 6M GPS. The SIM900 and GPS modules are powered separately to ensure stable operation and to avoid interference from other components. This issue can also be mitigated by connecting capacitors in parallel to the power lines for the SIM and GPS modules.

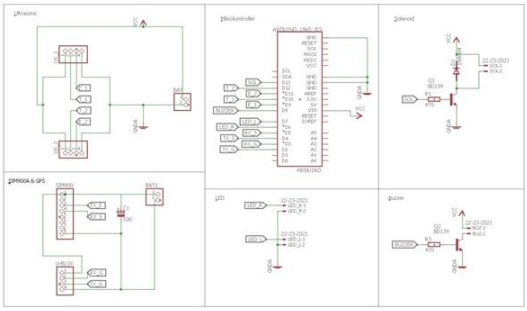

Figure 7. Circuit schematic

The output from the circuit includes two LEDs: a red LED to indicate the right side, and a yellow LED to indicate the rear side. The buzzer and solenoid lock are controlled using a BD139 transistor.

3. Result

The device testing was carried out in stages, starting with testing the transmission of GPS data to the database, lock mechanism testing, and blind spot detector testing.

The results of the blind spot detector testing were compared with measurement instruments, and the error was calculated using the Root Mean Square Error (RMSE) as shown in Eq. (1).

$$RMSE = \sqrt{\frac{\sum_{i=1}^{N}(Predicted_i - Actual_1)^2}{N}} \quad (1)$$

3.1 Testing the Transmission of GPS Data to the Database

At this stage, testing is conducted to verify the transmission of data from the microcontroller to the database, both in stationary and moving conditions, with data updates occurring every 2 minutes.

a. GPS Stationary Testing for 2 Hours

The purpose of this test is to evaluate the GPS's ability to successfully transmit location data to the database and to determine the accuracy level of the transmitted data.

Table 1. Stationary Condition Testing

No	Actual Data		Prediction Data		Error	
	Latitude	Longitude	Latitude	Longitude	Latitude	Longitude
1	-7.28208	112.78622	-7.281900	112.786290	-0.000181	-0.000066
2	-7.28208	112.78622	-7.281900	112.786290	-0.000181	-0.000066
3	-7.28208	112.78622	-7.281900	112.786290	-0.000181	-0.000066
4	-7.282	112.78626	-7.281900	112.786290	-0.000098	-0.000028
5	-7.282	112.78626	-7.281900	112.786290	-0.000098	-0.000028
6	-7.28201	112.78627	-7.281900	112.786290	-0.000111	-0.000020
7	-7.28199	112.78625	-7.281900	112.786290	-0.000092	-0.000043
8	-7.28201	112.78622	-7.281900	112.786290	-0.000109	-0.000066
9	-7.28201	112.78624	-7.281900	112.786290	-0.000109	-0.000066
10	-7.28201	112.78624	-7.281900	112.786290	-0.000106	-0.000051
11	-7.28199	112.78623	-7.281900	112.786290	-0.000094	-0.000059
12	-7.28199	112.78623	-7.281900	112.786290	-0.000094	-0.000059
Error					0.00012614	5.413E-05

International Journal of Electrical and Intelligent Engineering

In this test, the GPS was placed at a fixed point without any movement (i.e., the bicycle remained stationary). The test results are shown in Table 1.

Based on the error calculation using Eq. (1), the resulting error was 0.00012614% for latitude data and 5.413E-05% for longitude data. These values indicate a relatively small and stable error, suggesting that the data transmitted by the GPS is highly consistent with the data stored in the database.

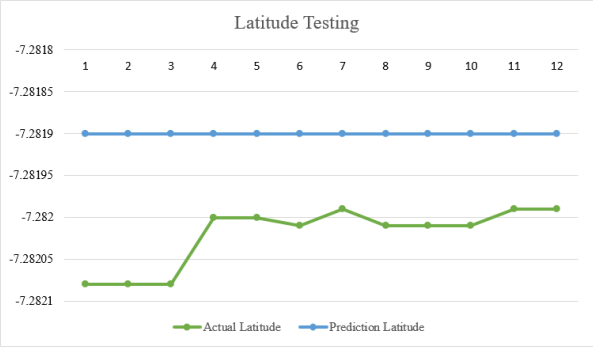

Figure 8. Latitude testing graph

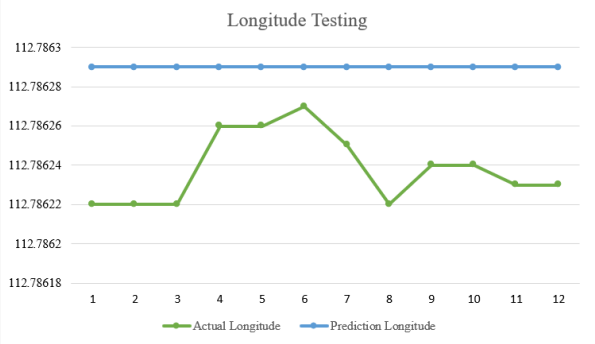

Figure 9. Longitude testing graph

Fig. 8 shows the comparison between Actual Latitude (green line) and Prediction Latitude (blue line) values in 12 tests. Actual Latitude fluctuates slightly from the 4th to the 12th point, with a range of values around -7.2821 to -7.2820 from the predicted latitude. This difference indicates that the prediction system has a deviation from the actual data, although on a very small scale. The discrepancy that occurs is relatively stable and does not show extreme spikes, which means that the model still has quite good performance in the context of location tracking.

Fig. 9 shows the comparison between Actual Longitude (green line) and Prediction Longitude (blue line) values during 12 tests. Actual Longitude fluctuates slightly from the 4th to the 11th test, with the peak occurring in the 6th test (around 112.78626) and the lowest value in the 8th test. However, the range of differences between the values is still very small (within four decimal places), indicating that the deviation between prediction and reality is not practically significant.

This graph confirms that the GPS system and data transmission are capable of providing stable and fairly accurate predictions, with a very small error rate—in line with what was mentioned previously (around 5.41295E-05%).

b. GPS Moving Test for 2 Hours

This test was conducted with the GPS in motion to assess the stability of data transmission while the bicycle was moving. The data was collected over a 2-hour journey without a specific route and at normal speeds (10–30 km/h). Table 2 shows the continuous changes in latitude and longitude values.

Table 2. Moving Condition Testing

Id	Latitude	Longitude
1	-7.282060	112.786244
2	-7.289599	112.780876
3	-7.326283	112.782608
4	-7/326288	112.782623
5	-7.326949	112.781829
6	-7.326949	112.781829
7	-7.326649	112.782722
8	-7.320558	112.791580
9	-7.320713	112.791664
10	-7.320713	112.791664
11	-7.320713	112.791748
12	-7.320646	112.791748

In the second test, where the GPS was in motion for 2 hours, the data shown in Table 2 continuously changed, indicating that the GPS successfully updated the position data to the database in real time.

3.2 Lock Mechanism Testing

In this stage, testing was conducted for the lock and unlock commands sent by the user through the website. The data is then stored in the database and read by the microcontroller. This test involved three conditions: Condition 1: Unlock command; Condition 2: Lock command; Condition 3: Activate alarm command.

International Journal of Electrical and Intelligent Engineering

Figure 10. The green LED lights up

Figure 11. The lock is unlocked

Figure 12. The red LED lights up

The testing of condition 1 (unlocking the padlock via the website) was successfully carried out, as indicated by the green LED on the device turning on, as shown in Fig. 10 and Fig. 11, confirming that the padlock was successfully unlocked. The time required to unlock the padlock—from the user command on the website to the successful unlocking—ranged from 10 to 25 seconds, depending on the server's gateway status.

The results for condition 2 (locking the padlock) also showed a similar response time of 10 to 25 seconds. A red LED on the device confirmed that the padlock was successfully locked, as shown in Fig. 12.

For condition 3, activating the alarm was also successful. The buzzer was triggered and sounded for 3 seconds, indicating that the alarm function worked as intended.

3.3 Blind Spot Detector Testing

At this stage, testing was carried out on the ultrasonic sensor readings, which function as a detector to monitor the actual blind spot conditions of the cyclist. The tests were conducted under four different scenarios detector testing against a wall, detector testing against a stationary vehicle, detector testing against a moving vehicle at a distance of 2 meters, detector testing against a moving vehicle at a distance of 4 meters. The detector testing setup is shown in Fig. 13

Figure 13. Detector testing setup

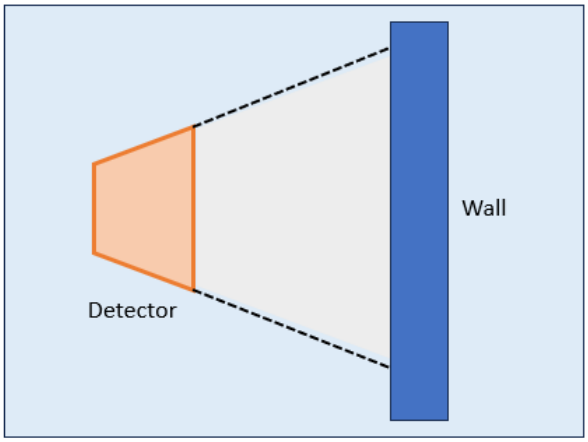

Figure 14. Detector Testing Setup Against a Wall

In the first test, the detector was directed toward a flat object (a wall) to evaluate the sensor's performance at distance intervals of 1 meter, as

Vol. 01, No. 01, July 2025 : 11-19 Received: June 24, 2025. Revised: July 10, 2025.

International Journal of Electrical and Intelligent Engineering

shown in Fig. 14. The experimental results are presented in Table 3.

Table 3. Detector Testing Against a Wall

No	Distance to Wall (cm)	Measured Distance (cm)	Error (%)
1	100	93.81	6.19
2	200	196.77	1.615
3	300	297.93	0.69
4	400	397	0.75
5	500	497.51	0.498
6	600	589.91	1.681
7	700	685.91	2.012
Average error			1.91964

Based on the results in Table 3, it can be observed that the detector performs optimally when aimed at flat surfaces. This is because the ultrasonic signal reflects ideally and matches expected calculations.

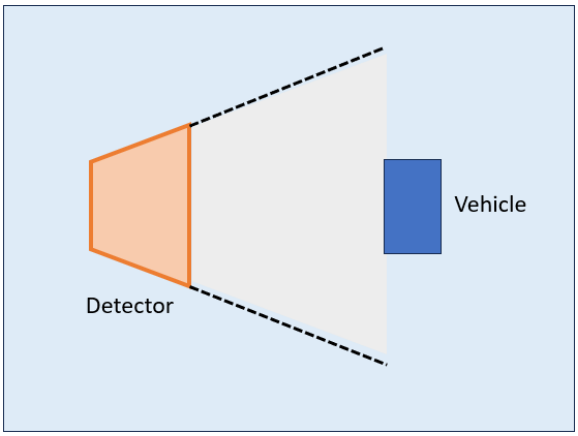

Figure 15. Detector Testing Setup Against a Vehicle

Table 4. Detector Testing Against a Stationary Vehicle at 1m

No	Distance to Vehicle (cm)	Measured Distance (cm)	Error (%)
1	100	116.15	16.15
2	200	202.91	1.455
3	300	305.55	1.85
4	400	475.80	18.95
5	500	580.90	16.18
6	600	698.91	16.48
7	700	116.15	16.15
Average error			12.46

The second test involved directing the detector at a stationary vehicle at a distance of 1 meter, as illustrated in Fig. 15. The results in Table 4 show that the detector faces challenges when detecting objects with irregular or non-flat surfaces. At distances beyond 0.3 meters, the detector's performance decreases, indicating that the reflected signal becomes distorted.

From previous tests showed the accuracy of detector testing against walls of 98% and testing against barrier vehicles of 87.54%. So the detector accuracy value is 92.77%.

The next test involved evaluating the detector's ability to detect a moving vehicle at distances of 2 meters and 4 meters, as shown in the testing setup in Fig. 16. The aim was to determine whether the detector could identify objects in the rider's blind spot.

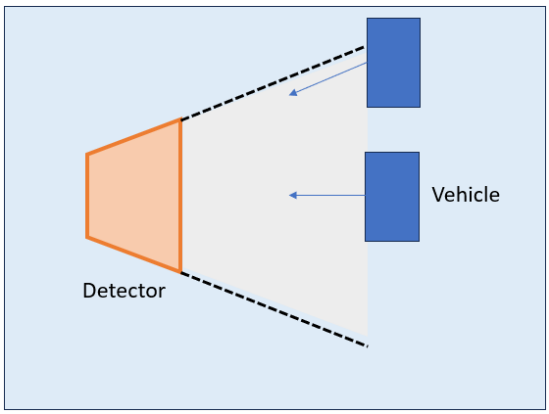

Figure 16. Detector Testing Setup with Moving Vehicle

Table 5 presents the results for testing the detector against a vehicle located 2 meters away on the right and rear sides. The data indicates that the detector functions ideally when the bicycle is moving at speeds of 10–40 km/h. At distances under 2 meters, the blind spot detection works effectively, and the LED and buzzer indicators are triggered when an object is within 1 meter.

Table 5. Detector Testing on Right and Rear Sides at 2m Distance

No	Velocity	Right-Side Indicator	Rear-Side Indicator	Buzzer
1	10 km/h	Active	Active	Active
2	20 km/h	Active	Active	Active
3	30 km/h	Active	Active	Active
4	40 km/h	Active	Active	Active

International Journal of Electrical and Intelligent Engineering

The final test involved placing a vehicle at a distance of 4 meters, using the same testing setup as in Fig. 13. The results are shown in Table 6. At this distance, the vehicle was no longer detected, as it exceeded the defined blind spot range. The detector performed well at speeds of 10–40 km/h. The LED indicator remained off at 4 meters but turned on at approximately 3 meters, while the buzzer was triggered when the object approached within 1 meter of the cyclist.

Table 6. Detector Testing on Right and Rear Sides at 4m Distance

No	Velocity	Right-Side Indicator	Rear-Side Indicator	Buzzer
1	10 km/h	Inactive	Inactive	Active
2	20 km/h	Inactive	Inactive	Active
3	30 km/h	Inactive	Inactive	Active
4	40 km/h	Inactive	Inactive	Active

4. Conclusion

After completing a series of stages—starting from system design and development, system testing, and system analysis—it can be concluded that the GPS coordinate data in a stationary condition showed an error value of 0.00012614% for latitude and 5.41295E-05% for longitude when compared to the actual coordinates. This indicates that the GPS module used is both optimal and precise. Meanwhile, the GPS coordinate data during movement, with data transmission every 10 minutes over a 2-hour journey, also remained consistent. The padlock, which is controlled via the website, successfully locked and unlocked, and the alarm functioned correctly according to the specified conditions. The blind spot detector operated optimally at a distance of 1–7 meters when facing a wall and 2 meters when detecting a moving vehicle traveling at 10–40 km/h.

From the results of this study, there are still several shortcomings and it is possible for further development, such as to achieve more ideal results than before, lidar or laser sensors can be used to detect irregularly shaped objects so that the detection results are more accurate.

Conflicts of Interest

The author declares that the data published in the manuscript does not constitute a conflict of interest with any party.

Author Contributions

1st and 2nd author conceived the ideas presented. All authors provided theory, performed calculations, verified the analysis methods, and discussed the results of the final manuscript.

References

[1] S. Darsini, “Tinjauan Sosiologis Tren Bersepeda di Tengah Pandemi Virus Corona,” Habitus: Jurnal Pendidikan, Sosiologi, & Antropologi, 2021.

[2] J. Park, O. S. Namkung and J. Ko, “Changes in Public Bike Usage After The COVID-19 Outbreak: A Survey of Seoul Public Bike Sharing Users,” Sustainable Cities and Society, vol. XCVI, pp. 104716-104716, 2023.

[3] C. C. Anderson, D. E. Clarkson, V. A. Howie, C. J. Withyman and C. Vandelanotte, “Health and well-being benefits of e-bike commuting for inactive, overweight people living in regional Australia,” Health Promotion Journal, vol. 33, pp. 349-357, 2023.

[4] D. R. Budi, R. Widyaningsih, L. Nur, B. Agustan, D. R. A. S. Dwi, W. Qohar and A. Asnaldi, “Cycling During COVID-19 Pandemic: Sport or Lifestyle,” International Journal of Human Movement and Sports Sciences, 2021.

[5] I. Hastanto, “Kecelakaan Lalu Lintas Meningkat, Tren Bersepeda di Kota Besar Jadi Kambing Hitam,” VICE Media, 2020.

[6] “Jumlah Korban Kecelakaan Lalu Lintas Menurut Jenis Kendaraan Bermotor di Provinsi DKI Jakarta,” Badan Pusat Statistik, DKI Jakarta, 2018.

[7] D. G. Pranata and J. Susanto, “Analisis Efektivitas Lajur Khusus Sepeda pada Kawasan Tomang-Cideng Timur,” JMTS: Jurnal Mitra Teknik Sipil, vol. IV, no. 1, pp. 13-22, 2021.

[8] R. G. Kusuma, Y. M. Devara, T. Handoyono and M. Arif, “Rancang Bangun Alat Blind Spot Area pada Kendaraan Truk Tangki Berbasis Mikrokontroler Arduino Uno,” Jurnal Keselamatan Transportasi Jalan, vol. VII, no. 1, pp. 1-7, 2020.

International Journal of Electrical and Intelligent Engineering

[9] A. C. Y. Tse, D. I. Anderson, V. H. L. Liu and S. Tsui, "Improving Executive Function of Children with Autism Spectrum Disorder through Cycling Skill Acquisition," Medicine & Science in Sports & Exercise, vol. 53, pp. 1417-1424, 2021.

[10] H. R. Zadry, H. A. Aziz, M. Widia, E. H. Sukadarin, H. Osman, Z. M. Jawi and M. A. Rahamn, "Traffic Accident in Indonesia and Blind Spot Detection Technology-An Overview," Human-Centered Technology for a Better Tomorrow, 2021.

[11] V. Ekroll, M. Svalebjørg, A. Pirrone, G. Böhm, S. Jentschke, R. v. Lier, J. Wagemans and A. Høye, "The illusion of absence: how a common feature of magic shows can explain a class of road accidents," Cogn. Research, vol. VI, no. 22, pp. 1-16, 2021.

[12] M. R. W. Pratama, M. Abdurohman and A. G. Putrada, "Vehicle Blind Spot Area Detection Using Bluetooth Low Energy and Multilateration," in 2021 9th International Conference on Information and Communication Technology (ICoICT), 2021.